

MECHANICS, POWER OUTPUT AND EFFICIENCY OF THE SWIMMING MUSKRAT (*ONDATRA ZIBETHICUS*)

BY F. E. FISH

Department of Biology, West Chester University, West Chester, PA 19380, U.S.A.

Accepted 4 November 1983

SUMMARY

The surface swimming of muskrats (*Ondatra zibethicus* Linnaeus) was studied by forcing individual animals to swim against a constant water current, of velocity ranging from 0.2 to 0.75 m s⁻¹, in a recirculating water channel. Lateral and ventral views of the swimming muskrats were filmed simultaneously for analysis of thrust by the propulsive appendages.

Drag measurements and flow visualization on dead muskrats demonstrated that these animals experience large resistive forces due to the formation of waves and a turbulent wake, because of the pressure and gravitational components which dominate the drag force.

Biomechanical analysis demonstrated that thrust is mainly generated by alternating strokes of the hindfeet in the paddling mode. A general lengthening of the hindfeet and presence of lateral fringe hairs on each digit increase the surface area of the foot to produce thrust more effectively during the power phase of the stroke cycle. Increased energy loss from drag on the foot during the recovery phase is minimized by configural and temporal changes of the hindfoot. Employing the models developed by Blake (1979, 1980*a,b*) for paddle propulsion, it was found that as the arc through which the hindfeet were swept increased with increasing velocity the computed thrust power increased correspondingly. However, the frequency of the stroke cycle remained relatively constant across all velocities at a level of 2.5 Hz.

Both mechanical and aerobic efficiencies rose to a maximum with increasing swimming velocity. The aerobic efficiency, which examined the transformation of metabolic power input to thrust power output reached a value of 0.046 at 0.75 m s⁻¹. The mechanical efficiency expressing the relationship of the thrust power generated by the paddling hindfeet and laterally compressed tail (Fish, 1982*a,b*) to the total mechanical power developed by the propulsive appendages increased to a maximum of 0.33 at 0.75 m s⁻¹.

I conclude that the paddling mode of swimming in the muskrat is relatively inefficient when compared to swimming modes which maintain a nearly continuous thrust force over the entire propulsive cycle. However, the paddling mode permits the muskrat to generate propulsive forces effectively while swimming at the surface. The evolution of this mode for semi-aquatic mammals represents only a slight modification from a terrestrial type of locomotion.

Key words: Muskrat, mechanics, swimming.

INTRODUCTION

Swimming in aquatic vertebrates is accomplished either by undulations of the body and tail or by movements of the paired appendages through rowing, paddling and subaqueous flight (Robinson, 1975). Most of the research on the mechanics and energetics of swimming has focused on various piscine species employing an undulatory propulsive mode (see review by Webb, 1975*a*). This research has added much to the understanding of the dynamics of fish swimming, but has ignored the alternate modes of swimming exhibited in secondarily aquatic animals.

Recently, Blake (1979, 1980*a*) has formulated several models to determine the power output produced in paddling locomotion. These models were found to be applicable to the study of paddle propulsion in a small semi-aquatic mammal, the muskrat (*Ondatra zibethicus*). This rodent swims at the surface by alternate paddling motions of the hindfeet (Howell, 1930; Kirkwood, 1931; Svihla & Svihla, 1931; Mizelle, 1935; Dagg & Windsor, 1972).

The power input expressed as the metabolic rate of the surface swimming muskrat has been previously reported (Fish, 1982*b*). The ratio of the mechanical power output to metabolic power input determines the efficiency of energy utilization. Combining a biomechanical analysis of the paddling mode of the muskrat with physiological data allows an integrated approach to the study of aquatic adaptation.

Additionally, the muskrat affords the opportunity to examine the consequences of surface swimming. The forces encountered at the air-water interface for non-piscine vertebrates are complex and larger than those of submerged swimmers. Thus surface swimming may be expected to influence the energy budget of the muskrat due to the energy lost to surface waves formed by the animal (Herte!, 1966; Schmidt-Nielsen, 1972).

MATERIALS AND METHODS

Experimental animals

Ten muskrats (nine male and one female) were live-trapped in Ingham Co., Michigan, during the spring and summer of 1978 and 1979. The mean body mass of the muskrats was 649 g (range 530–1604 g) over the test period. The animals were maintained outdoors in large, concrete ponds at the Limnology Research Laboratory on the campus of Michigan State University. The ponds were approximately 2 m deep, allowing unrestricted swimming and diving. Abundant aquatic vegetation, which grew in the ponds, was readily consumed by the muskrats and used for bedding material. The diet was supplemented with apples. The ponds were equipped with platforms above the water. Nest boxes were provided on the platforms and modified for the capture of a single animal when needed for testing.

Water channel

Experiments on swimming were conducted in a recirculating water channel, based on a design by Vogel & LaBarbera (1975) and previously described and illustrated by Fish (1982*b*). A working section was provided in the channel in which a single muskrat

was allowed to swim without interference. The width and depth of the muskrat relative to the dimensions of the water channel represented 30 and 29 %, respectively. The upstream end of the working section was bounded by a plastic grid (commercially termed 'egg crate') in conjunction with a 5 cm wide grid of plastic straws, which removed turbulence from the water flow. The downstream end of the working section was bounded by a low voltage electrified grid that stimulated swimming by the muskrat. Wires attached to the grid ran along the floor of the working section to prevent the animal from standing on the floor to rest. The voltage was controlled with a Powerstat (Superior Electric Co.). All electricity was disconnected from the grid when the muskrat maintained steady swimming. During high speed trials, a removable wall was placed in the working section *to* constrict its cross-sectional area and thus increase the water velocity. The top of the working section was formed by a Plexiglas metabolic chamber, which was used for the measurement of oxygen consumption as has been reported previously (Fish, 1982*b*).

Water velocity (U) was controlled either by a Sears 25 electric fishing motor (Model No. 217.590091) or by a Mercury electric outboard motor (Model No. 10019) situated in the return channel. Power to the motor was provided by a 12 V storage battery connected *to* a 6 A battery charger. Motor speed was related to water speed, determined by the time a drop of ink or neutrally buoyant particle traversed a given distance. Because muskrats swimming against the water current appeared to remain stationary relative to their position in the water channel, the water velocity and swimming speed were assumed to be equivalent.

Kinematic analysis

The muskrats were tested at velocities ranging from 0.2 to 0.75 m s⁻¹. There was no sequence order of the test velocities for each muskrat. Single animals were forced to swim steadily at a given test velocity for a period of 10 to 30 min.

Plexiglas windows were installed in the side and floor of the working section to allow for observation and filming. The windows were marked with a grid of 2 cm squares to act as reference points. To film simultaneous lateral and ventral views of the muskrat, a mirror was positioned under the floor at a 45° angle to reflect the ventral image of the animal toward the camera.

Individual muskrats swimming over the range of velocities were filmed at 24 and 50 frames s⁻¹ with a Bolex H-16 SB reflex ciné camera equipped with a Kern Vario-Switar 100 POE zoom lens (1:1.9, $f = 16\text{--}100\text{mm}$) using 16mm film (Kodak 4-X Reversal film 7277, ASA 320). The camera was driven with an ESM 13 V d.c. motor. Lighting was supplied by three 250 W flood lamps surrounding the working section. For analysis, sequential tracings of the propulsive appendages were made from films using a stop-action projector (Lafayette Instrument Co., Model 00100).

Modifications of the models proposed by Blake (1979, 1980*a,b*) were used to compute the power, energy and efficiency generated by the paddling appendages of the muskrat from the kinematic data obtained from the films. The stroke cycle of the hindfeet was analysed according to the assumptions stated by Blake (1979) for drag-based paddling propulsion. Unlike in the blade-element theory used by Blake, all forces were estimated from a point on the foot, designated as the centre of action (CA), which approximated to the point where the mean force would act.

*Drag measurements and **Flow** visualization*

Total body drag was measured on seven dead muskrats, which were frozen into a natural swimming posture with the tail stretched out straight. The hindlegs were removed for separate drag measurements. When placed in the water each carcass was buoyed up by residual air in the lungs, air entrapped in the fur and the lowered density of the frozen tissues, so that the muskrat floated at a level similar to living animals, when compared to the films of swimming muskrats.

All drag measurements were made using a lever type balance (Fig. 1). Six metal bars were positioned orthogonally and welded to a central point. The bars in the rotational axis (Z) acted as a fulcrum and passed through two sets of bearings held in position by brackets. The ends of the bars in the horizontal axis (X) were threaded for balancing weights which could be positioned to align the vertical axis bars (Y) at

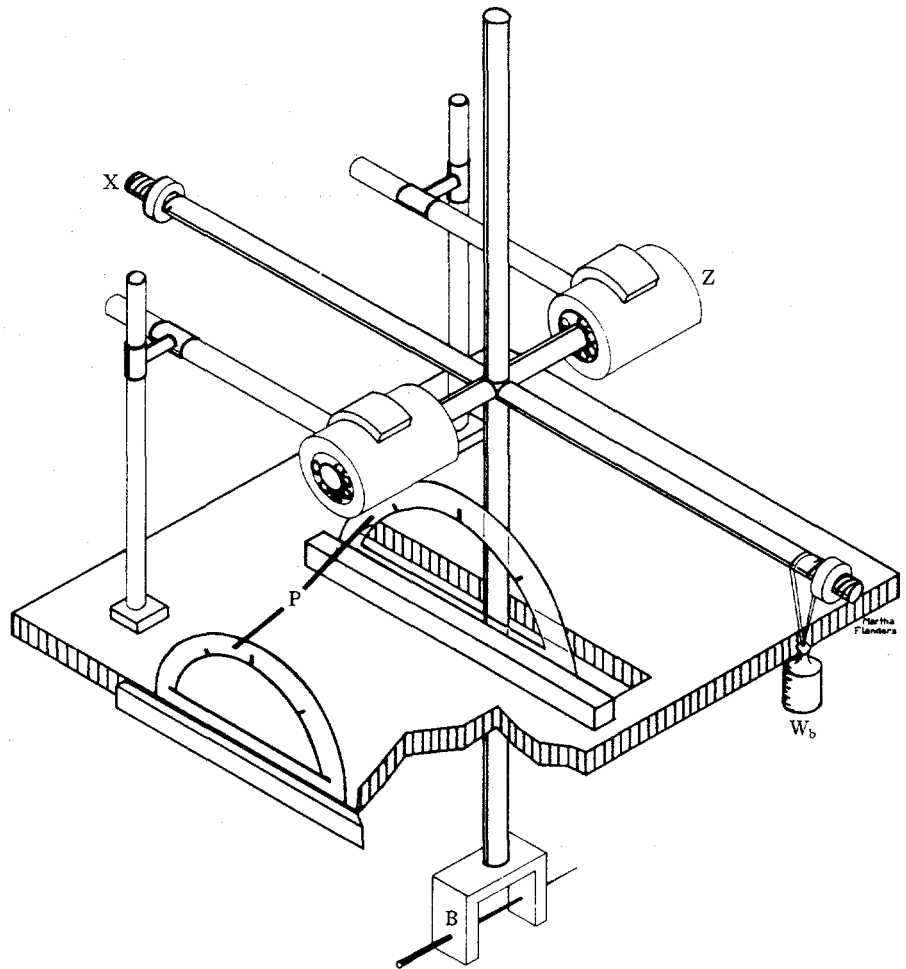


Fig. 1. Drag balance. The three axes are indicated by X, Y and Z. W_b represents the counterbalancing weight, B, the mounting bracket used to hold the muskrat and P, the protractors. Procedure for use of the drag balance is given in the text.

90° with the protractors (P). The lower bar of the vertical axis was employed as the mounting bar for the attachment of the muskrat body. At the end of the mounting bar was a plastic bracket (B) shaped as an inverted U. The ends of the bracket straddled the nose of the muskrat and a large pin was passed through holes in the bracket and through the nose of the animal. This arrangement firmly attached the animal to the mounting bar while allowing rotation of the muskrat about the long axis of the pin, but prevented yawing.

When placed in the water current, a torque developed around the rotational axis due to the drag on the muskrat. The drag was countered by a sliding weight (W_b) on the horizontal axis bar. The weight was moved to a point on the bar such that the vertical axis bar was orientated at 90° as determined by siting the vertical axis with the two protractors. By measuring the distances from the fulcrum to the pin and the weight, a standard lever equation was used to compute the drag in Newtons. Since the mounting bar was not submerged, no correction for drag was necessary.

The drag of isolated hindfeet was measured in a manner similar to that described above. However, the feet were attached directly to the mounting bar. The hindfeet had been frozen in either a fully spread or fully closed position, similar to the positions of the feet during the stroke cycle in the power and recovery phases, respectively. The feet were positioned so that the plantar surface of the power phase foot and dorsal surface of the recovery phase foot were normal to the incident water flow. Additionally, drag measurements of the power phase foot were determined with the fringe hairs removed to determine their effect on thrust. The drag on the submerged portion of the mounting bar was subtracted from the foot drag.

Frontal and plantar surface areas of the isolated hindfeet were measured from photocopies using a portable area meter (LAMBDA Instruments Corp., Model LI-3000).

The water flow around the body of a single dead muskrat at 0.3 and 0.6 m s⁻¹ was observed by the injection of a water-soluble ink into the flow through five small diameter tubes (0.7 mm, i.d.). The tubes were positioned in front of the muskrat and along its sides and posterior end.

Statistical procedure

Statistical analyses were made with reference to Steele & Torrie (1960). In order to perform the statistical analyses for the various data sets, trials on muskrats were assumed to be independent of one another. Variation about means was expressed as \pm one standard error (s.e.). Non-linear data were logarithmically transformed for statistical analysis.

RESULTS

Biomechanics

Kinematics were analysed on muskrats swimming steadily at velocities from 0.25 to 0.75 m s⁻¹. At 0.2 m s⁻¹, the experimental animals did not swim steadily. Instead, they accelerated toward the front of the working section and then drifted in the current toward the downstream end. Although this motion was sufficient for metabolic determinations (Fish, 1982*b*), motion analysis was confined to the higher velocities.

Muskrats swam as in the description of Mizelle (1935). They swam at the water surface maintaining a slightly lordotic posture. However, some muskrats were observed to flex their backs, although this was never observed in animals swimming unrestricted in ponds. The forelegs of the muskrats were held under the chin with the feet flexed, so that the plantar surfaces were directed dorsally under the antebrachium. Short pawing motions, which did not generate thrust, were sometimes observed, but were highly irregular.

The hindfeet moved in a paddling mode as has been observed by others (Howell, 1930; Kirkwood, 1931; Svihla & Svihla, 1931; Mizelle, 1935; Dagg & Windsor, 1972). Robinson (1975) has defined paddling as the movement of a paddle antero-posteriorly in a vertical plane parallel to the direction of motion of the craft. For the muskrat, the paddling mode is facilitated by alternating strokes of the hindfeet. The paddling cycle consisted of power and recovery phases (Fig. 2).

During the power phase (Fig. 2; frames 15–21), the hindfoot was accelerated posteriorly through an arc by plantarflexion of the foot, flexion of the shank and retraction of the femur. Although the major paddling motion occurred at the ankle joint, movement of the femur by retraction increased the posterior velocity of the foot by as much as 0.18 m s^{-1} . Maximum velocity of the hindfoot was attained when orientated at approximately 90° to the horizontal. At the end of the power phase, rapid

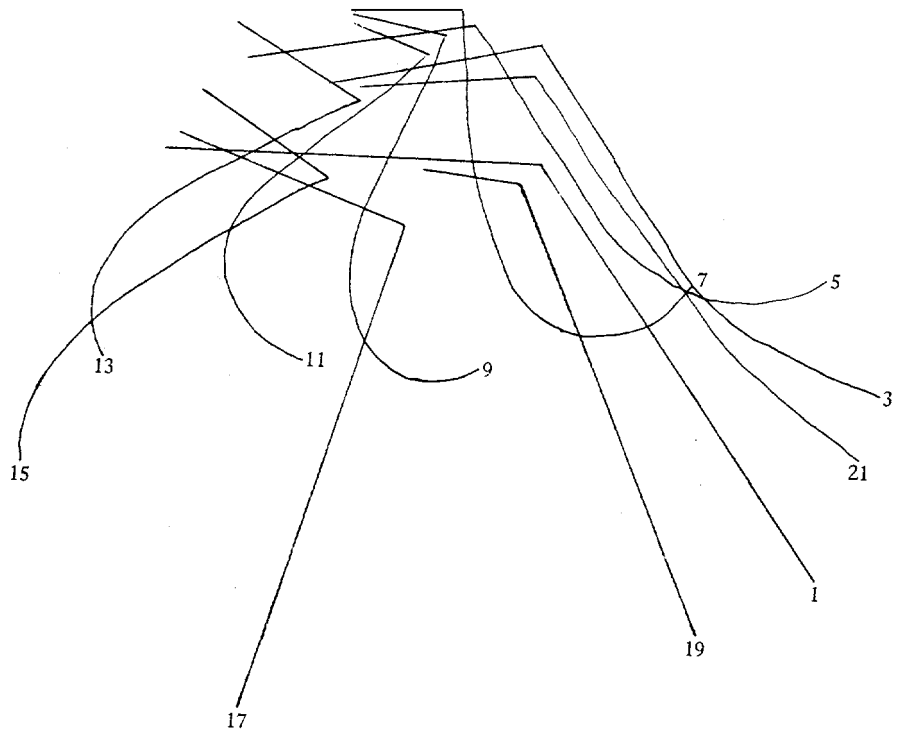


Fig. 2. Diagrammatic representation of the lateral view of the hindfoot through the stroke cycle. The alternate sequential frames are indicated by the numbers for each foot position, where the power phase is indicated by frames 15–21 and the recovery phase by frames 5–13. The segments of the foot shown are the phalanges, metatarsals, tarsals and tibia. $U = 0.45 \text{ m s}^{-1}$; 50 frames s^{-1} .

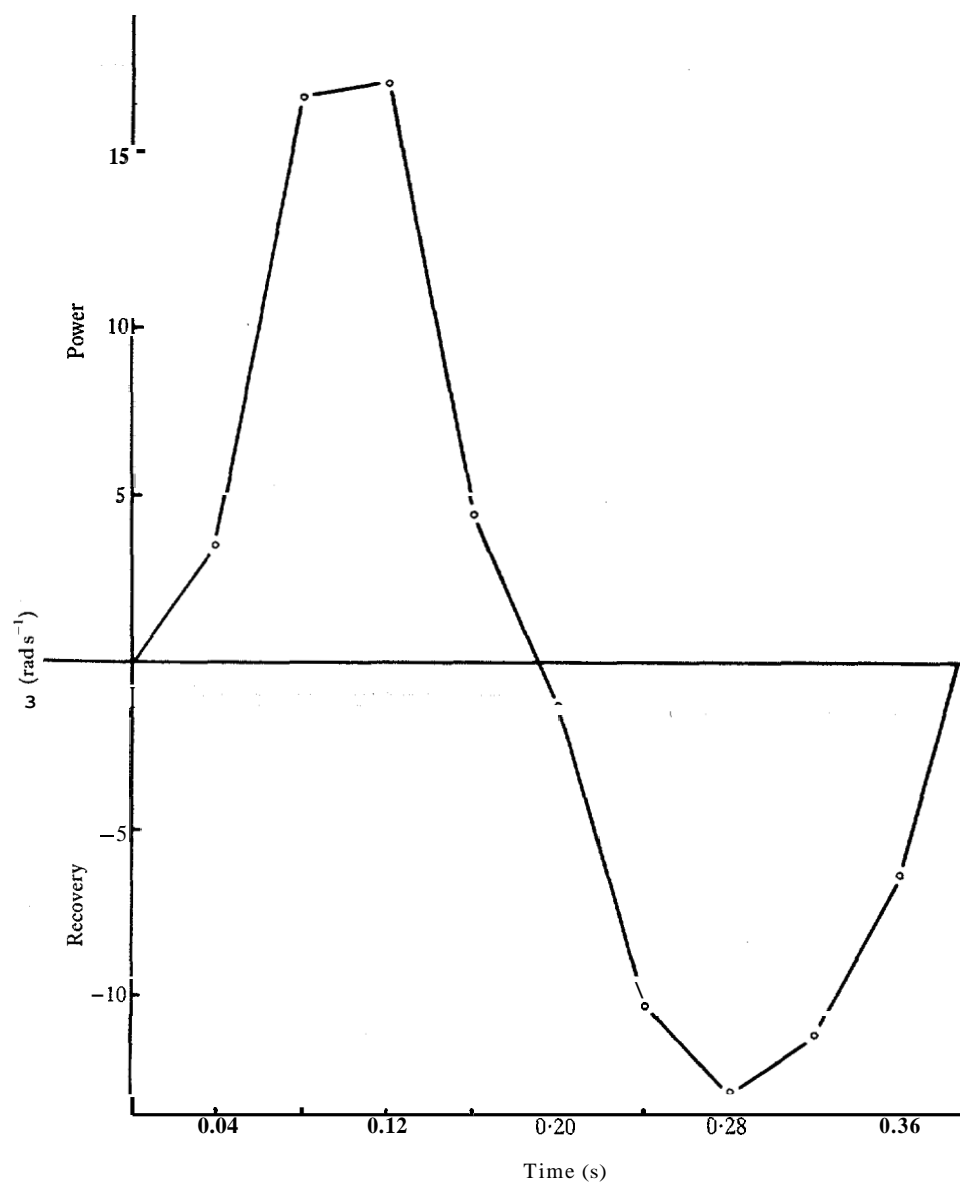


Fig. 3. The angular velocity (ω) of the power and recovery phases of the hindfoot as plotted over the time of one stroke cycle for a muskrat swimming at 0.45 m s^{-1} . The angular velocity was defined as the arc in radians swept by the metatarsals of the foot divided by the time for either power or recovery phases.

deceleration of the hindfoot approximated the rate of acceleration at the beginning of the phase (Fig. 3).

During the power phase, the digits were extended and maximally abducted so that they were fully spread and the foot was slightly pronated. Although there is only a slight webbing between the bases of the digits, it appears that the lateral fringe of stiff hairs, each 3–7 mm long, is passively erected by the resistance of the water as the foot

is swept posteriorly. The effective plantar surface area including fringe hairs (mean: 15.7 cm^2 ; $N = 7$) was 21% higher than the same feet with the fringe hairs removed (mean: 12.5 cm^2 ; $N = 7$).

The recovery phase of the stroke cycle (Fig. 2; frames 5–13) was characterized by dorsiflexion and supination of the hindfoot, plantarflexion of the digits, protraction of the femur and extension of the shank. The angular velocity of the recovery phase foot showed an acceleration to a maximum at 90° to the long axis of the body and then a deceleration at the end of the phase (Fig. 3). The maximum angular velocity of the recovery phase was on average 9% lower than that of the power phase.

The frontal surface area of the hindfoot during the recovery phase was reduced to a mean value of 7.1 cm^2 ($N = 7$) by adduction and flexion of the digits and supination of the foot. A similar motion has been observed in grebes (Peterson, 1968).

Fig. 4 illustrates the frequency of the stroke with respect to U . The frequency remained relatively constant over all velocities at $2.5 \pm 0.06 \text{ Hz}$. This was similar to

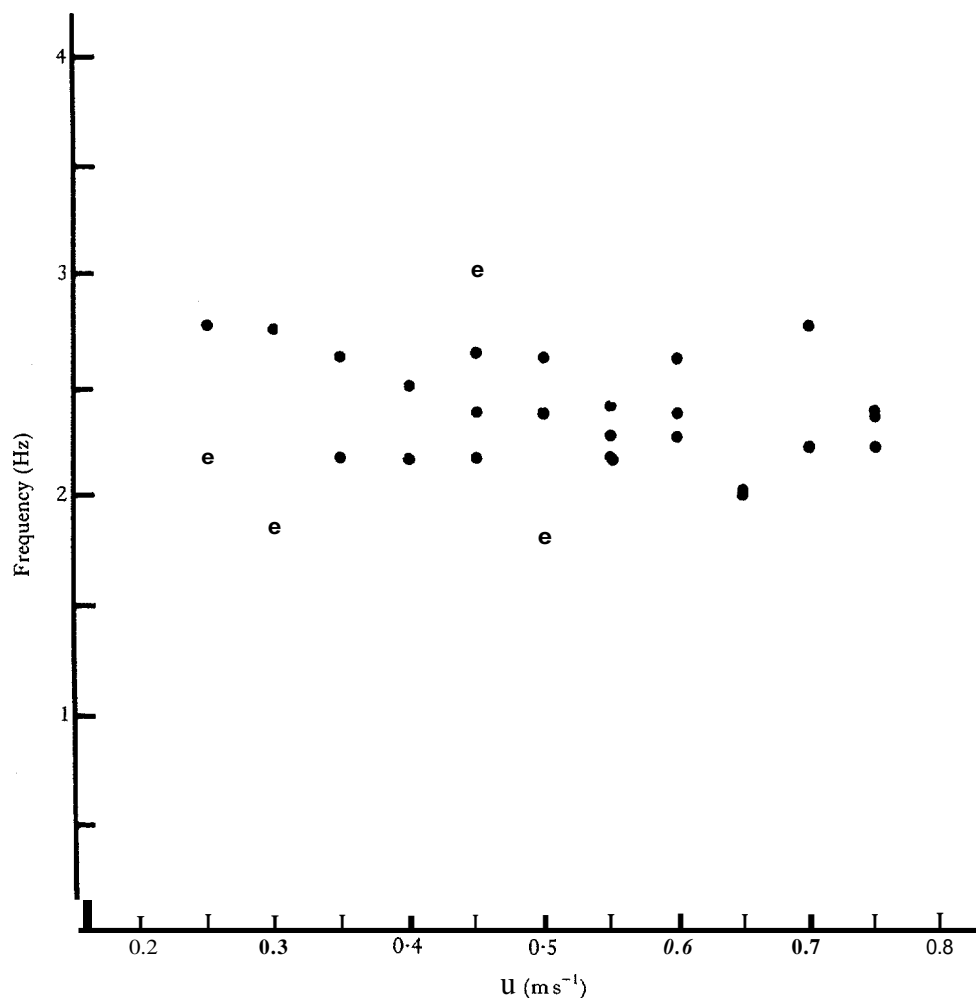


Fig. 4. The stroke frequency of the hindfeet as a function of the swimming velocity, U .

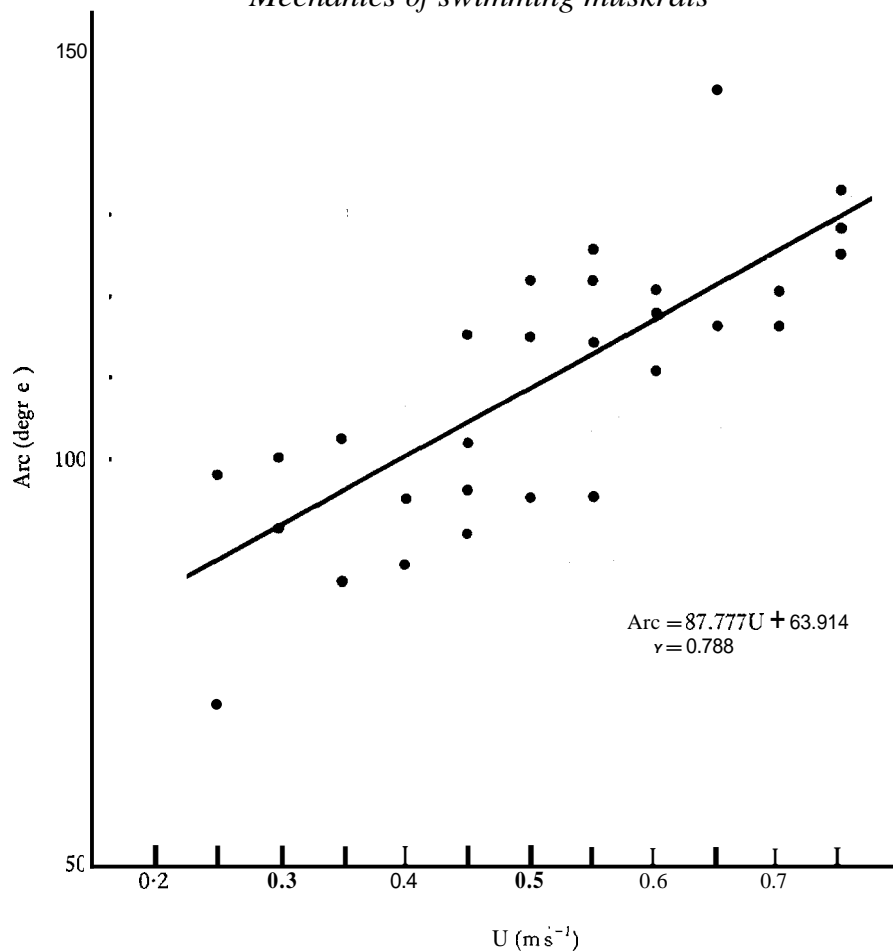


Fig. 5. The arc of the hindfoot plotted as a function of the swimming velocity, U .

the constant stroke frequency seen in swimming ducks (Prange & Schmidt-Nielsen, 1970), minks (Williams, 1983) and competitive human swimmers (Nadel, 1977). However, this differs from previous observations on the muskrat, beaver, nutria and mink (Mordvinov, 1976), sea lion (Kruse, 1975) and fish (Bainbridge, 1958; Hunter & Zweifel, 1971; Videler, 1981), in which the frequency of the propulsive appendages increased with swimming speed.

The stroke cycle of the muskrat was asymmetrical in time. The mean durations of power and recovery phases were 0.18 ± 0.01 and 0.22 ± 0.01 s, respectively, over the range of U . The duration of the power phase was significantly shorter than the recovery phase ($P < 0.0005$; paired t-test; $df = 28$).

The arc through which the hindfeet were swept during the power phase measured as the angle between the metatarsals and horizontal plane is shown as a function of U in Fig. 5. The arc varied linearly with U , so that the muskrat increased swimming speed by increasing the distance the hindfeet were swept in a constant time period. The arc was only increased at the end of the phase, while at the beginning the foot

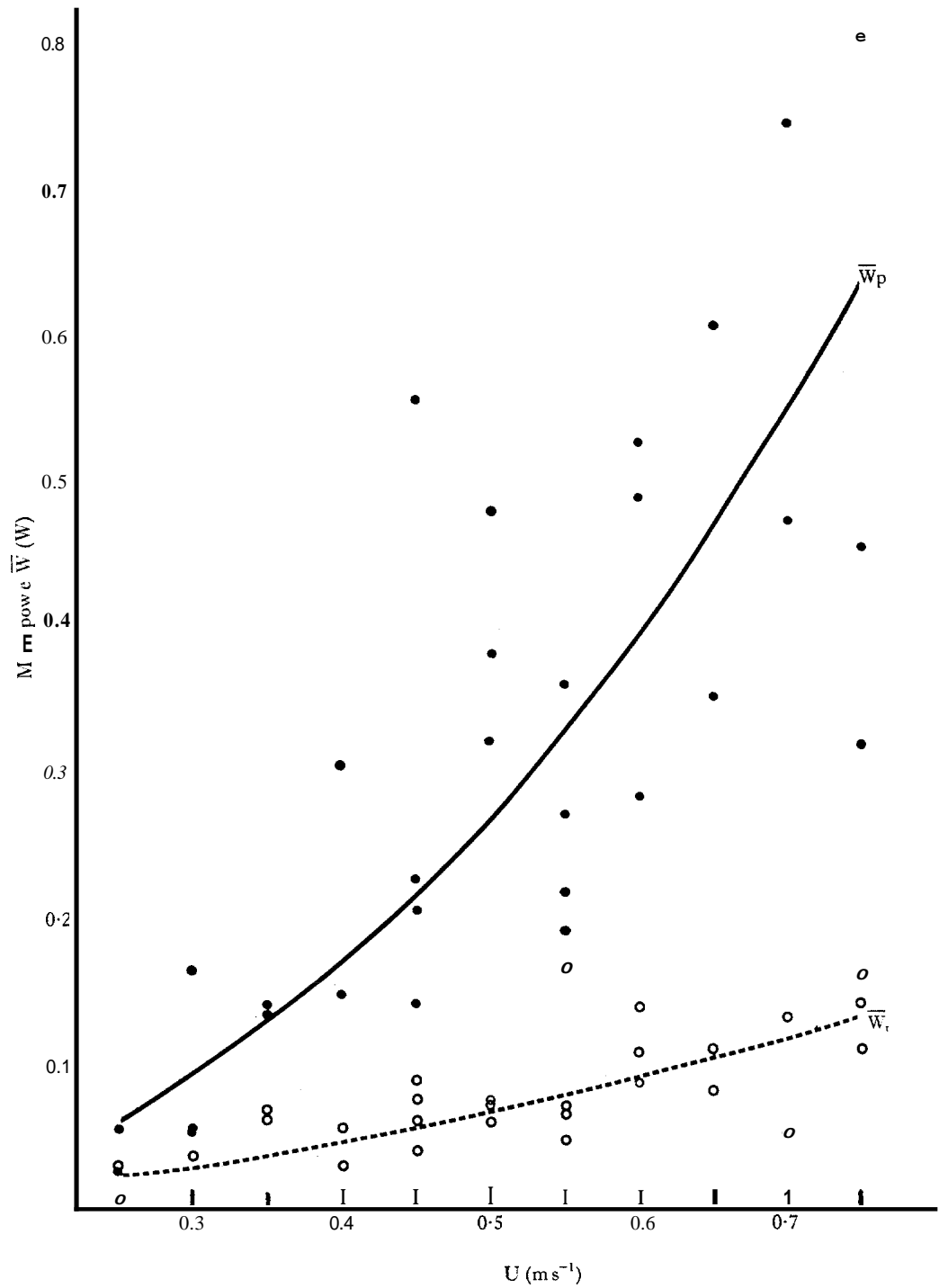


Fig. 6. The mean power produced by the muskrat during the power (\bullet — \bullet) (\bar{W}_p), $\bar{W}_p = 1.17U^{2.12}$ and recovery (\circ — \circ) (\bar{W}_r), $\bar{W}_r = 0.20U^{1.50}$, phases for one paddle as a function of the swimming velocity, U.

initiated the stroke at a relatively constant angle of 24° from 0.25 to 0.55 m s^{-1} , which decreased slightly at higher velocities.

The energy and power generated for both power and recovery phases were computed from the equations by Blake (1979). For the recovery phase, the sign was changed to positive in equation (1) (Blake, 1979) to calculate the resultant relative velocity to adjust for the direction change of the foot.

CA was represented for the power and recovery phases by the distal end of the second metatarsal of the foot. The CA, which could be easily observed from the films, averaged 5.2% and never more than 28% of the true centre of thrust determined by blade-element analysis.

The effective radius of rotation for the paddle was estimated by the method utilized by Youm, McMurtry, Flatt & Gillespie (1978) and outlined by Alexander (1983).

Using the model presented by Blake (1979), the mean power expended for the

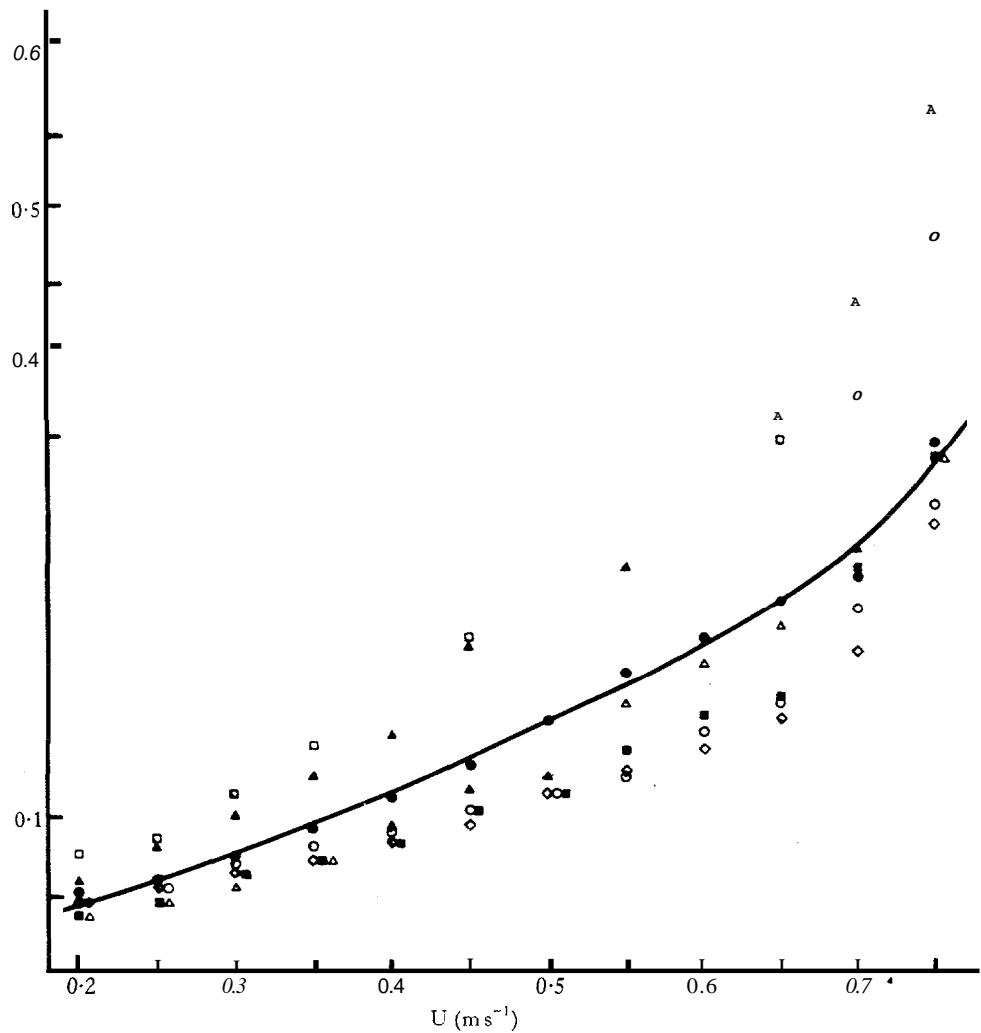


Fig. 7. Drag as function of water velocity, U . Symbols indicate drag for individual muskrats.

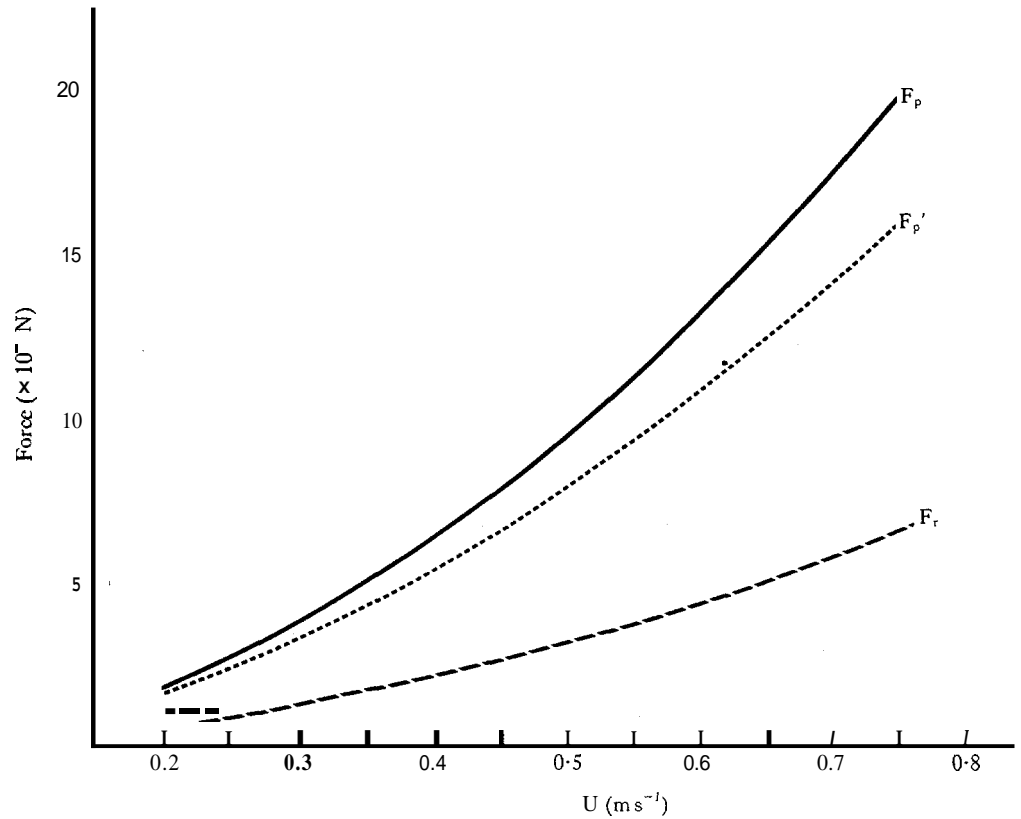


Fig. 8. The force on isolated hindfeet determined by drag measurements in the power phase (F_p), power phase with fringe hairs removed (F_p'), and recovery phase (F_r) plotted against the water flow velocity, U .

power and recovery phases of a single hindfoot was calculated (Fig. 6). A curvilinear increase of the mean power expended over the range of test velocities was noted for both power and recovery phases. Regressions of the data for the power and recovery phases (Fig. 6) were highly significant ($P < 0.001$) with correlation coefficients of 0.85 and 0.80 ($df = 27$), respectively. The mean power expended during the recovery phase represented 20–39% of the power expended in the power phase over the range of U .

Drag and flow visualization

The drag experienced by the muskrat body over the range of U is shown in Fig. 7. The drag increased curvilinearly with increasing U with the larger animals having higher drag. This was expressed by the equation:

$$\text{Drag} = 0.46U^{1.48}.$$

The correlation coefficient was found to be 0.9 ($N = 7$), which was significant at $P < 0.001$.

The importance of increased surface area from the fringe hairs is illustrated in Fig. 8. At the same water flow velocities, U , the normal force which was measured

on the drag balance for the isolated hindfeet with the fringe hairs intact, was 20% higher than without the hairs. During the recovery phase, the configuration change of the hindfoot represented a reduction of 55% from the frontal surface area of the hindfoot (including the fringe hairs) during the power phase. As a consequence of the reduced frontal surface area, the drag for the recovery phase of the hindfoot represented only 33% of the drag experienced by the foot in the power phase position (Fig. 8).

Ink injected into the water flow just anterior to the muskrat accumulated under the nose, indicating a large stagnation point with a high pressure (Potter & Foss, 1975). The presence of a bow wave anterior to the muskrat indicated the same phenomenon. Much of the ink was swept under the body and encountered large turbulence due to the flow separation which occurred posterior to the deepest part of the body at speeds greater than 0.6 m s^{-1} .

Turbulence along the side of the muskrat was observed at 0.3 and 0.6 m s^{-1} . Turbulence with the development of vortices occurred approximately midway along the body.

The greatest turbulence appeared just downstream of the posterior end of the muskrat at both velocities. Similar data have been gathered on live muskrats by Mordvinov (1974). The observed turbulence allowed water to cross over the tail. Both in the region of the tail and further downstream, the wake of the muskrat showed a considerable amount of turbulence and vorticity.

Water flow about isolated hindfeet in the power phase showed large amounts of turbulence directly downstream. Similar results were observed for feet positioned in the recovery phase.

DISCUSSION

Blake (1979, 1980a) was able to calculate the energy utilized for propulsion by the paddling movements of the pectoral fins of an angelfish (*Pterophyllum eimekei*). The energy was determined as the difference between work done in the power and recovery phases of both fins through the stroke cycle.

The work done by the paddling of the muskrat for forward propulsion was calculated as the sums of differences of the energies in Joules generated by power and recovery phases of the stroke cycle of both hindfeet. Added to this quantity was the small energetic contribution generated by the lateral undulations of the tail (Fish, 1982a, Fig. 3). Empirically, the sum of energies producing the muskrat's forward motion (E_{th}) was found to correspond to the regression equation (Fig. 9):

$$E_{th} = 0.35U^{2.11},$$

which was significant at $P < 0.001$ with a correlation coefficient of 0.84 ($df = 27$).

Over the range of U , E_{th} was 2.2 – 3.2 times greater than E_D , where E_D represents the propulsive energy expended due to body drag. E_D was calculated as the product of the drag, U , and the time of the stroke cycle. Such a difference between these two independent estimations was probably due to the movements of the propulsive appendages and acceleration of the body, which were not taken account of in the estimation of E_D . This has also been a primary problem preventing correspondence between similar measures in fish (Webb, 1975a).

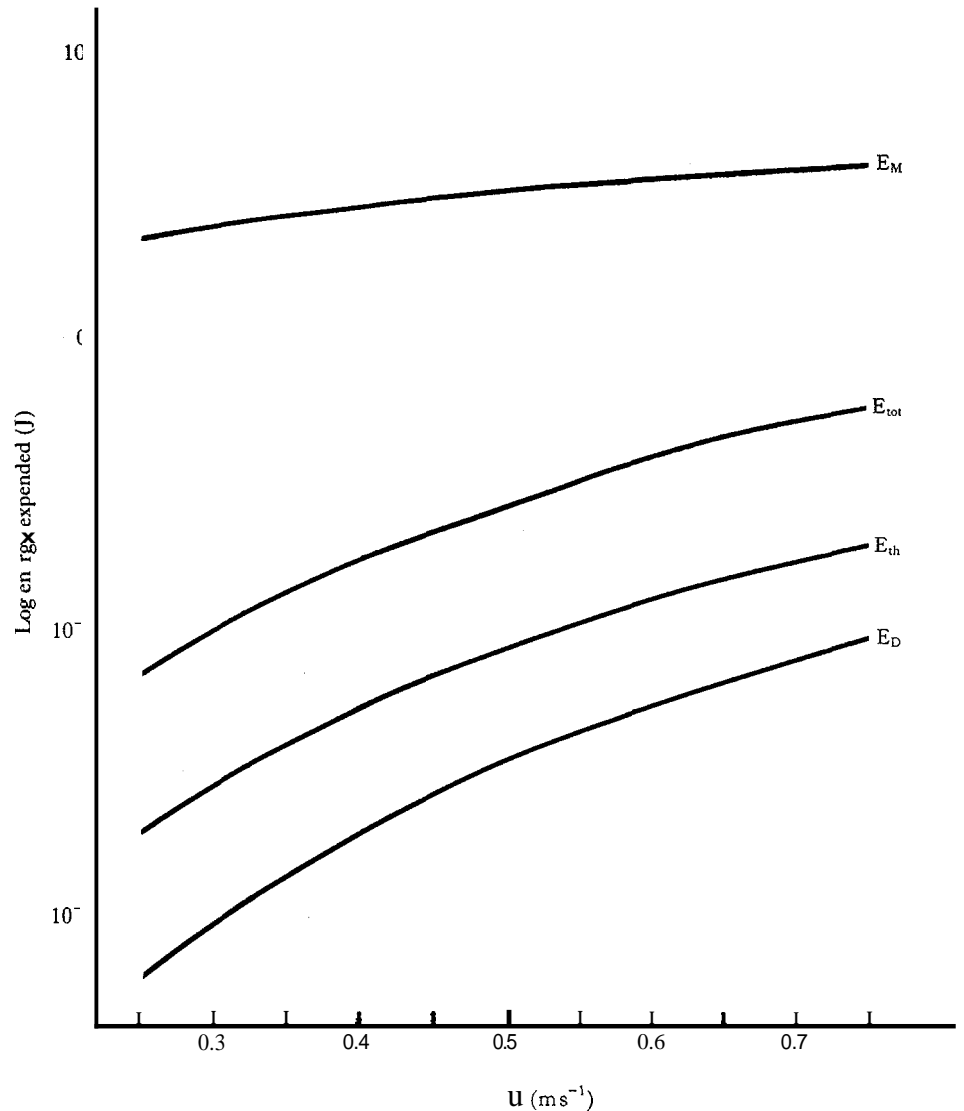


Fig. 9. Comparison of the logs of energies expended at various swimming velocities, U . E_M is the metabolic expenditure, E_{tot} is total energy generated by the paddling hindfeet and undulating tail, E_{th} is the total energy generated which produces thrust, and E_D is the energy lost to drag on the body.

The energy utilized for forward propulsion (E_{th}) does not represent the total energy expended in paddling. The total energy required for power and recovery phases to produce the hydrodynamic thrust force (E_p and E_r , respectively) was calculated from the integration of equation (13) in Blake (1979).

Additionally, the energy losses required for the inertia and added mass of the hindfeet, and undulations of the tail were calculated. The energy required to move the mass of the hindfoot (9.36 g) during the power (E_f) and recovery (E_f') phases was computed from the integration of equation (17) of Blake (1979). The energy needed to accelerate and decelerate the added mass (power, E_a ; recovery, E_a') was calculated

from equation (22) of Blake (1979), using the maximum chord of the foot for each phase (power, 0.04 m; recovery, 0.01 m). The total energy produced by the tail over the stroke cycle (E_t) was calculated from Fish (1982a).

The efficiency of energy utilization for the swimming muskrat may be analysed from three perspectives. These are the metabolic thrust efficiency (η_{aerob}), overall energetic efficiency (η_e) and mechanical efficiency (η_{me}).

The metabolic thrust efficiency for the swimming muskrat was computed by :

$$\eta_{\text{aerob}} = E_{\text{th}}/E_M,$$

where E_M in Joules is calculated from the regression equation for the total mass specific metabolic rate at 25 °C in Fish (1982b, Table 1A) multiplied by the mean mass of the muskrats, the caloric conversion factor of 20.1 J ml O_2^{-1} , the stroke cycle time in seconds, and divided by 3600s (Fig. 9). The η_{aerob} was found to increase steadily to a measured peak value of 0.046 at 0.75 m s^{-1} (Fig. 10).

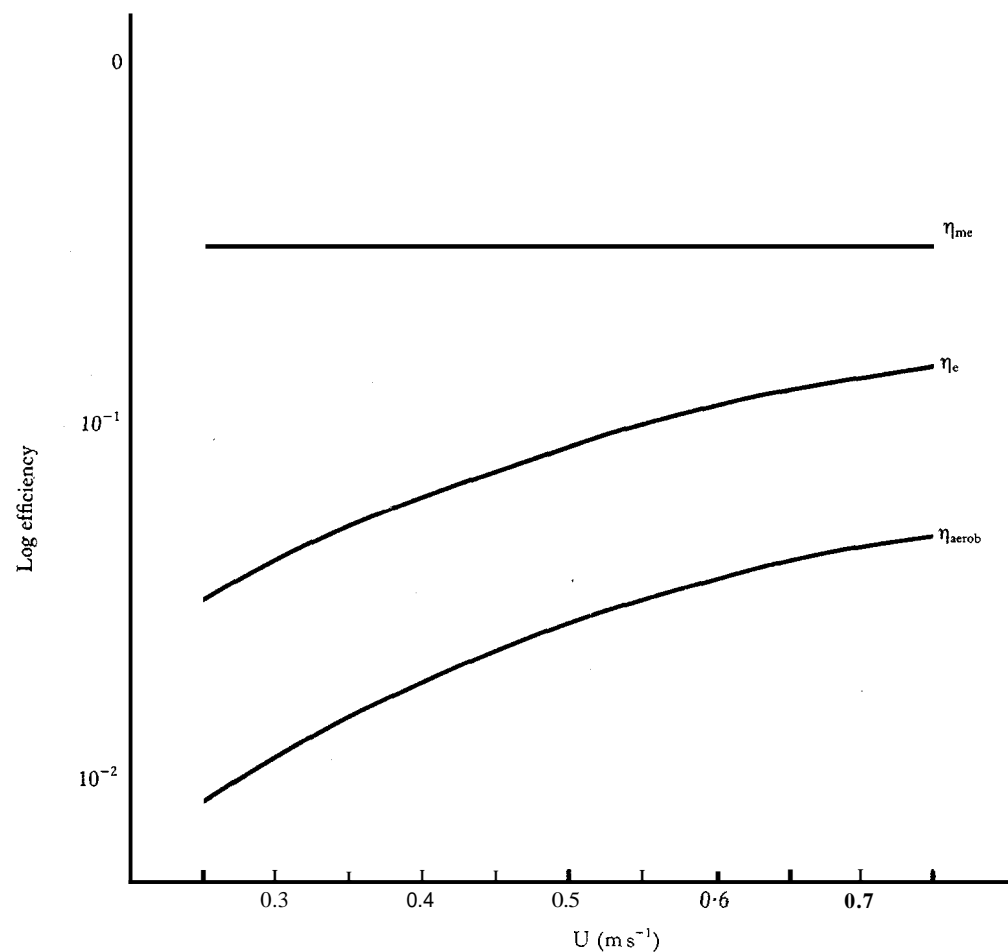


Fig. 10. The logs of efficiencies as a function of swimming velocity, U . η_{me} represents the mechanical efficiency, η_e the overall energetic efficiency and η_{aerob} the metabolic efficiency.

The overall energetic efficiency was calculated as the ratio of the sum of energies expended by the tail and two hindfeet during the stroke to the metabolic energy and is given by :

$$\eta_e = E_{\text{tot}}/E_M,$$

where E_{tot} was computed by:

$$E_{\text{tot}} = 2(E_p + E_r + E_f + E_a + E_f' + E_a') + E_u.$$

The relationship between E_{tot} and U (Fig. 9) is:

$$E_{\text{tot}} = 1.02U^{1.94},$$

which was significant at $P < 0.001$ with a correlation coefficient of 0.88 ($df = 27$).

As illustrated in Fig. 10, the value of η_e was found to increase steadily with increasing U . With regard to the metabolic thrust efficiency, the overall energetic efficiency was 2.5–3.9 times larger. This difference was due to the additional energy needed during the stroke for the recovery phase and the acceleration and deceleration of the hindfeet which is not taken into account in the computation of the η_{aerob} .

Webb (1975*b*) calculated η_{aerob} for rainbow trout and sockeye salmon as 0.15 and 0.22, respectively. Unlike organisms that propel themselves by lateral undulations, paddle-propulsive organisms, such as the muskrat, are not as efficient in the conversion of metabolic energy to propulsive power. For paddlers such as the duck (Prange & Schmidt-Nielsen, 1970), minks (Williams, 1983) and humans (DiPrampo, Pendergast, Wilson & Hennie, 1974) maximum values for η_{aerob} were 0.047, 0.014 and 0.052, respectively.

Prange (1976) found that η_{aerob} for green sea turtles reached a maximum value of 0.09. This high value is not too surprising since the sea turtle derives thrust in power and recovery phases of the forelimb stroke (Walker, 1971). Comparable efficiencies of 0.12 and 0.13 were found for the fish *Cymatogaster*, which utilizes a lift-based propulsive mechanism (Webb, 1975*b*). These values are believed to be lower than efficiencies of caudal fin propulsors due to the energy necessary for rotating and accelerating the pectoral appendages (Webb, 1975*b*).

The mechanical efficiency is computed by:

$$\eta_{\text{me}} = E_{\text{th}}/E_{\text{tot}},$$

and is illustrated in Fig. 10 over the range of U . With increasing U , η_{me} increased steadily from 0.27 to 0.33. The maximum value for the muskrat was 2.1 times higher than the mechanical efficiency of fish using labriform locomotion (Blake, 1980*a*). Blake reported an 11% reduction in the efficiency from the power to recovery phase. In the case of the muskrat, the energy expended in the recovery phase and from the added mass was responsible for a significant reduction in η_{me} . In the angelfish frictional drag dominated in the recovery phase, but in the muskrat, high pressure drag during the recovery phase of the muskrat expended relatively more energy.

In contrast to fish which swim in the carangiform mode, the muskrat is inefficient in the generation of propulsive power. The mechanical efficiency of the rainbow trout and sockeye salmon were 0.7 and 0.9, respectively (Webb, 1975*b*). Wu (1971) has suggested that under optimal conditions the propulsive efficiency for this type of fish

may be as high as 97%. It thus appears that the paddling mode with its recovery phase and associated energy loss is a liability in the attainment of high propulsive efficiency.

The muskrat's morphology is little different from that of a terrestrial form. The most significant morphological change in terms of propulsion has been the development of large, fan-shaped hindfeet with lateral fringe hairs and a laterally compressed tail.

During paddling locomotion, the paddle must be shaped so as to maximize its drag as it is swept posteriorly in order to maximize thrust and efficiency. The optimum paddle shape is similar to a flat plate orientated normal to the direction of movement so that the water striking the paddle surface produces drag (Robinson, 1975). Blake (1981) found that fish which employ drag-based propulsion are more likely to have triangular fins which generate large pressure drag.

In mammals, the surface areas of the hindfeet, which are used as paddles, is increased by interdigital webbing (e.g. otter, beaver) or fringe hairs (e.g. muskrat), in conjunction with a general lengthening of the foot. Howell (1930) stated that the percentage of hindfoot length to body length for terrestrial rodents is usually less than 20%, while a value of 38.5% was reported for the muskrat.

Howell (1930) believed that fringe hairs were not as efficient as webbing, but were undoubtedly adequate to propel a small body. In comparison to webbing, fringe hairs would not serve as an effective barrier in preventing water from passing between the digits, thereby reducing the effective surface area of the foot. However, Counsilman (1968) reported that a human hand with the fingers spread slightly produced more drag than a closed hand. Such results may be induced by an increase in turbulence between the digits increasing pressure drag (Counsilman, 1968). The muskrat may therefore utilize the fringe hairs to generate turbulence for more effective propulsion. The significance of the fringe hairs was illustrated in the present study by a large decrease of the drag on isolated hindfeet in which the hairs were removed.

Alexander (1983) has argued that generation of thrust is most economical when the mass of water being worked on is large. The effective increase in surface area by modifications of the muskrat foot would therefore accelerate a large mass of water posteriorly, providing momentum to the animal.

In contrast to the power phase, in which the drag on the hindfoot should be maximized, the recovery phase should reduce the drag on the foot as much as possible. In this manner, the thrust generated during the power phase will not be cancelled during the recovery phase. Observations on the recovery phase of the muskrat showed an adduction and plantarflexion of the digits, and supination of the entire foot. These actions tended to minimize the frontal surface area of the foot, thus reducing drag.

Although the muskrat has evolved a foot morphology which allows it to move in an aquatic environment while maintaining terrestrial capabilities, it has been necessary to change in gait from a terrestrial type to one which is more effective for swimming. In contrast to terrestrial vertebrates, in which the recovery phase is shorter than the power phase (Goslow, Reinking & Stuart, 1973; Edwards, 1976), the muskrat has a relatively longer recovery phase. The recovery phase for terrestrial locomotion is 'wasted' time, and a shorter recovery would maximize the time that the limb contacts the substrate for more effective propulsion (Edwards, 1976). Because the muskrat foot during recovery has a large pressure drag and relative velocity, a long recovery

would reduce the resultant velocity and decrease the negative thrust force. The negative thrust would also be minimized by a decrease in the radius of the recovery phase through a shift of CA due to plantarflexion of the digits and retraction of the femur to bring CA closer to the rotation point.

Because of the metabolic and mechanical inefficiencies of the paddling mode and substantial energy loss to the wake for surface swimming, aquatic locomotion is more costly for the muskrat than for more highly adapted organisms. However, in that the muskrat is semi-aquatic and is thus highly mobile on both land and water, the morphology of this animal should be viewed as a compromise of both form and function between vastly different environments.

I wish to express my sincere appreciation to Dr J. L. Edwards, Dr P. W. Webb, Dr R. W. Hill and Dr R. H. Baker for their advice and constructive criticism during the course of this study. I also wish to thank especially Dr R. W. Blake for assistance with his model and E. Rybak for programming assistance. Dr C. D. McNabb, Dr R. A. Pax, Dr G. W. Bird and J. L. Erwin are gratefully acknowledged for use of facilities and M. Flanders for assistance with figures. I am grateful to the Department of Zoology, Michigan State University for financial support and to the American Society of Mammalogists and Sigma Xi for funding through student grants-in-aid. The State of Michigan, Department of Natural Resources is acknowledged for allowing the collection of muskrats.

REFERENCES

- ALEXANDER, R. McN. (1983). *Animal Mechanics*. Oxford: Blackwell Scientific Publications.
- BAINBRIDGE, R. (1958). The speed of swimming of fish as related to size and to frequency and amplitude of tail beat. *J. exp. Biol.* **35**, 109–133.
- BLAKE, R. W. (1979). The mechanics of labriform locomotion. I. Labriform locomotion in the angelfish (*Pterophyllum eimekei*): an analysis of the power stroke. *J. exp. Biol.* **82**, 255–271.
- BLAKE, R. W. (1980a). The mechanics of labriform locomotion. II. An analysis of the recovery stroke and the overall fin-beat cycle propulsive efficiency in the angelfish. *J. exp. Biol.* **85**, 337–342.
- BLAKE, R. W. (1980b). Mechanics of drag-based mechanisms of propulsion in aquatic vertebrates. In *Vertebrate Locomotion: Symposia of the Zoological Society of London*, No. 48, (ed. M. H. Day), pp. 29–52. London: Academic Press.
- BLAKE, R. W. (1981). Influence of pectoral fin shape on thrust and drag in labriform locomotion. *J. Zool., Lond.* **194**, 53–66.
- COUNSILMAN, J. W. (1968). *The Science of Swimming*. N. J.: Prentice-Hall.
- DAGG, A. I. & WINDSOR, D. E. (1972). Swimming in northern terrestrial mammals. *Can. J. Zool.* **50**, 117–130.
- DIPRAMPERO, P. E., PENDERGAST, D. R., WILSON, D. W. & HENNIE, D. W. (1974). Energetics of swimming in man. *J. appl. Physiol.* **37**, 1–5.
- EDWARDS, J. L. (1976). A comparative study of locomotion in terrestrial salamanders. Ph.D. dissertation, University of California, Berkeley.
- FISH, F. E. (1982a). Function of the compressed tail of surface swimming muskrats (*Ondatra zibethicus*). *J. Mammal.* **63**, 591–597.
- FISH, F. E. (1982b). Aerobic energetics of surface swimming in the muskrat *Ondatra zibethicus*. *Physiol. Zool.* **55**, 180–189.
- GOSLOW, G. E., JR., REINKING, R. M. & STUART, D. G. (1973). The cat step cycle: hind limb joint angles and muscle lengths during unrestrained locomotion. *J. Morph.* **141**, 1–41.
- HERTEL, H. (1966). *Structure, Form and Movement*. New York: Rheinhold.
- HOWELL, A. B. (1930). *Aquatic Mammals*. Springfield, Illinois: C. C. Thomas.
- HUNTER, J. R. & ZWEIFEL, J. R. (1971). Swimming speed, tail beat frequency, tail beat amplitude and size in jack mackerel, *Trachurus synnetrucys*, and other fishes. *Fishery Bull. Fish Wildl. Serv. U.S.* **69**, 253–266.
- KIRKWOOD, F. C. (1931). Swimming of the muskrat. *Mammal.* **12**, 317–318.
- KRUSE, D. H. (1975). Swimming metabolism of California sea lions, *Zalophus californianus*. M.S. thesis, San Diego State University.

- MIZELLE, J. D. (1935). Swimming of the muskrat. *J. Mammal.* **16**, 22–25.
- MORDVINOV, Y. E. (1974). The character of boundary layer in the process of swimming in the muskrat (*Ondatra zibethica*), and mink (*Mustela lutreola*). *Zool. Zh.* **53**, 430–435 (in Russian).
- MORDVINOV, Y. E. (1976). Locomotion in water and the indices of effectiveness of propelling systems for some aquatic mammals. *Zool. Zh.* **55**, 1375–1382 (in Russian).
- NADEL, E. H. (1977). Thermal and energetic exchanges during swimming. In *Problems with Temperature Regulation during Exercise*, (ed. E. R. Nadel), pp. 91–119. New York: Academic Press.
- PETERSON, R. T. (1968). *The Birds*. New York: Time Inc.
- POTTER, M. C. & FOSS, J. F. (1975). *Fluid Mechanics*. New York: Ronald Press.
- PRANGE, H. D. (1976). Energetics of swimming of a sea turtle. *J. exp. Biol.* **64**, 1–12.
- PRANGE, H. D. & SCHMIDT-NIELSEN, K. (1970). The metabolic cost of swimming in ducks. *J. exp. Biol.* **53**, 763–777.
- ROBINSON, J. A. (1975). The locomotion of plesiosaurs. *N. Jb. Geol. Palaont. Abh.* **149**, 286–332.
- SCHMIDT-NIELSEN, K. (1972). Locomotion: energy cost of swimming, flying and running. *Science, N.Y.* **177**, 222–228.
- STEELE, R. G. D. & TORRIE, J. H. (1960). *Principles and Procedures of Statistics*. New York: McGraw-Hill.
- SVIHLA, A. & SVIHLA, R. D. (1931). The Louisiana muskrat. *J. Mammal.* **12**, 12–28.
- VIDELER, J. J. (1981). Swimming movements, body structure and propulsion in cod *Gaudus morhua*. In *Vertebrate Locomotion: Symposia of the Zoological Society of London*, No. 48, (ed. M. H. Day), pp. 1–27. London: Academic Press.
- VOGEL, S. & LABARBERA, M. (1978). Simple flow tanks for research and teaching. *Bioscience* **28**, 638–643.
- WALKER, W. F., JR. (1971). Swimming in sea turtles of the family Cheloniidae. *Copeia* **1971**, 229–233.
- WEBB, P. W. (1975a). Hydrodynamics and energetics of fish propulsion. *Bull. Fish. Res. Bd Can.* **190**, 1–159.
- WEBB, P. W. (1975b). Efficiency of pectoral-fin propulsion of *Cymatogaster aggregata*. In *Swimming and Flying in Nature*, Vol. 2, (eds T. Y. Wu, C. J. Brokaw & C. Brennen), pp. 573–584. New York: Plenum Press.
- WILLIAMS, T. M. (1983). Locomotion in the North American mink, a semi-aquatic mammal. I. Swimming energetics and body drag. *J. exp. Biol.* **103**, 155–168.
- WU, T. Y. (1971). Swimming of a waving plate. *J. Fluid Mech.* **10**, 321–344.
- YOUM, Y., McMURTRY, R. Y., FLATT, A. E. & GILLESPIE, T. E. (1978). Kinematics of the wrist. I. An experimental study of radial-ulnar deviation and flexion-extension. *J. Bone Jt Surg.* **60A**, 423–431.